

Chapter 4

Characterization and Solubilization of Pyrrole–Imidazole Polyamide Aggregates

The text of this chapter was taken in part from a manuscript co-authored with Amanda E. Hargrove, Jevgenij A. Raskatov, Jordan L. Meier, and Peter B. Dervan (California Institute of Technology)

(Hargrove, A. E.; Raskatov, J. A.; Meier, J. L.; Montgomery, D. C.; Dervan, P. B. "Characterization and Solubilization of Pyrrole–Imidazole Polyamide Aggregates," *J. Med. Chem.* **2012**, 55, 5425-5432)

Abstract

To optimize the biological activity of pyrrole–imidazole polyamide DNA-binding molecules, we characterized the aggregation propensity of these compounds through dynamic light scattering and fractional solubility analysis. Nearly all studied polyamides were found to form measurable particles 50–500 nm in size under biologically relevant conditions, while HPLC-based analyses revealed solubility trends in both core sequences and peripheral substituents that did not correlate with overall ionic charge. The solubility of both hairpin and cyclic polyamides was increased upon addition of carbohydrate solubilizing agents, in particular, 2-hydroxypropyl- β -cyclodextrin (Hp β CD). In mice, the use of Hp β CD allowed for improved injection conditions and subsequent investigations of the availability of polyamides in mouse plasma to human cells. The results of these studies will influence the further design of Py-Im polyamides and facilitate their study in animal models.

Introduction

N-methylpyrrole (Py) and N-methylimidazole (Im) polyamides are heterocycle-based oligomers that bind the minor groove of DNA in a sequence-specific manner.¹⁻³ Investigations of Py-Im polyamide biological properties have demonstrated that these compounds are cell permeable,³⁻⁵ localize to the nucleus,³⁻⁵ and display transcriptional inhibition, likely through an allosteric mechanism by disrupting the transcription factor-DNA interface.^{6,7} This compression may be responsible for the observed reduction in transcription factor occupancy upon polyamide-DNA complexation.⁸⁻¹⁰ Gene regulation properties have been illustrated in cell culture models targeting transcription factors androgen receptor (AR),⁸ glucocorticoid receptor (GR),¹⁰ hypoxia inducible factor (HIF),^{9,11} nuclear factor kappaB (NF- κ B),¹² AURKA/AURKB,¹³ and TGF- β .^{14,15} We have investigated the utility of Py-Im polyamides in organismal models through *in vitro* ADMET studies,¹⁶ real-time biodistribution monitoring methods,¹⁷ and, most recently, the development of mouse pharmacokinetic and toxicity profiles.¹⁸ Recent efforts to develop more potent polyamides, however, have been hindered by poor solubility.¹⁹ These observations raise concerns about the likely aggregation of Py-Im polyamides. If aggregation is an issue, how does particle size correlate with structural features such as size, charge, shape, turn substitution, and Py/Im composition of the oligomer?

Recent studies of the aggregation of small molecule drug candidates through dynamic light scattering (DLS) and detergent-based assays have highlighted the importance of such considerations in drug design.²⁰⁻²³ Indeed, a screen of over 70,000 potential drug candidates by Shoichet and co-workers found that 95% of the initial hits acted as aggregate-based inhibitors.²⁴ At the same time, several currently approved drugs

can be classified as aggregate-based inhibitors²⁵ and in some cases aggregate particle size may be linked to pharmaceutical efficacy.^{23,26,27} We thus decided to investigate this important pharmacokinetic parameter and its relationship to the biological activity of Py-Im polyamides. As our laboratory explores the efficacy of polyamides in animal disease models, there becomes a pressing need to characterize the aggregation and solubility properties of these compounds as well as to investigate the use of formulating reagents to solubilize polyamides at the high concentrations required for animal injections.

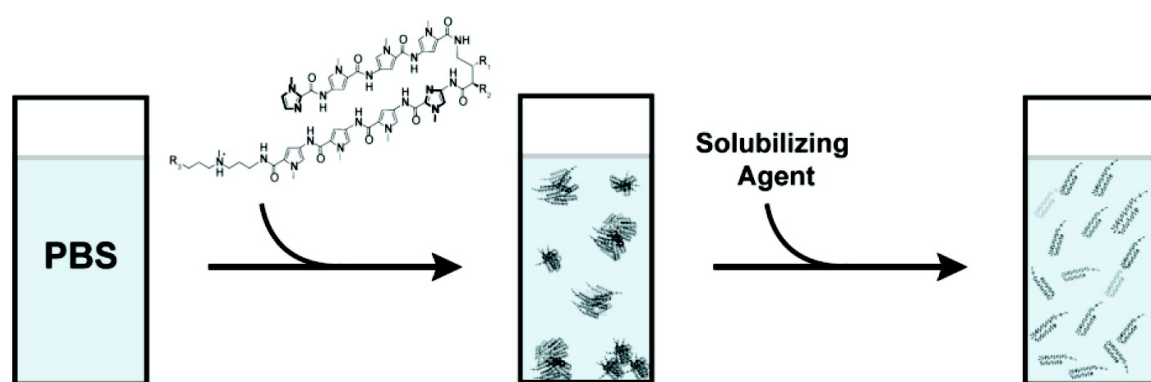


Figure 4.1: The use of solubilizing agents can disrupt the aggregation of polyamides and allow increased solubility.

Results and Discussion

Selection of a Panel of Polyamides

We selected two libraries of Py-Im hairpin polyamides, **1-6** and **7-11**, targeting the AR/GR consensus sequence 5'-WGWCW-3' (W = A/T)^{8,28} or the NF-κB consensus sequence 5'-WGGWW-3', respectively (Figure 4.2).¹²

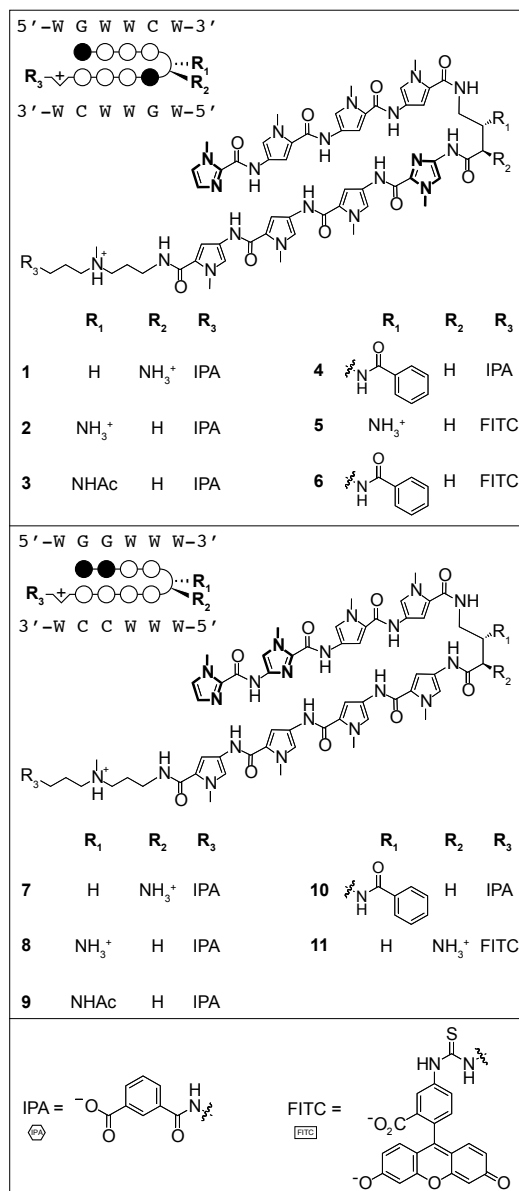


Figure 4.2 Chemical structures of hairpin polyamide library along with the corresponding circle-stick models and target DNA sequences. Legend: Black circle = Im; white circle = Py; semi-circle = γ -aminobutyric acid unit with dashed (R , β) or wedge (R , α) substituents; hexagon = isophthalic acid / IPA; rectangle = fluorescein / FITC; W = A/T bases.

These two different heterocyclic cores were diversified with a variety of substituents at the 4-aminobutyric acid (GABA) turn positions (R_1 , R_2) and the C-terminal tail position (R_3). Substituents at these positions are known to affect DNA binding and biological activities.^{19,29,30} In addition, the employment of cyclic polyamide architectures has resulted in increased DNA binding affinities and selectivities³¹ as well as improved efficacy against AR-regulated genes.²⁸ Taken in context with our recent finding of increased murine toxicity of cyclic polyamides,¹⁸ we decided to also investigate the properties of cycles **12-14** (Figure 4.3). All Py-Im polyamides were synthesized according to previously published solid-phase procedures.^{12,18,19,32}

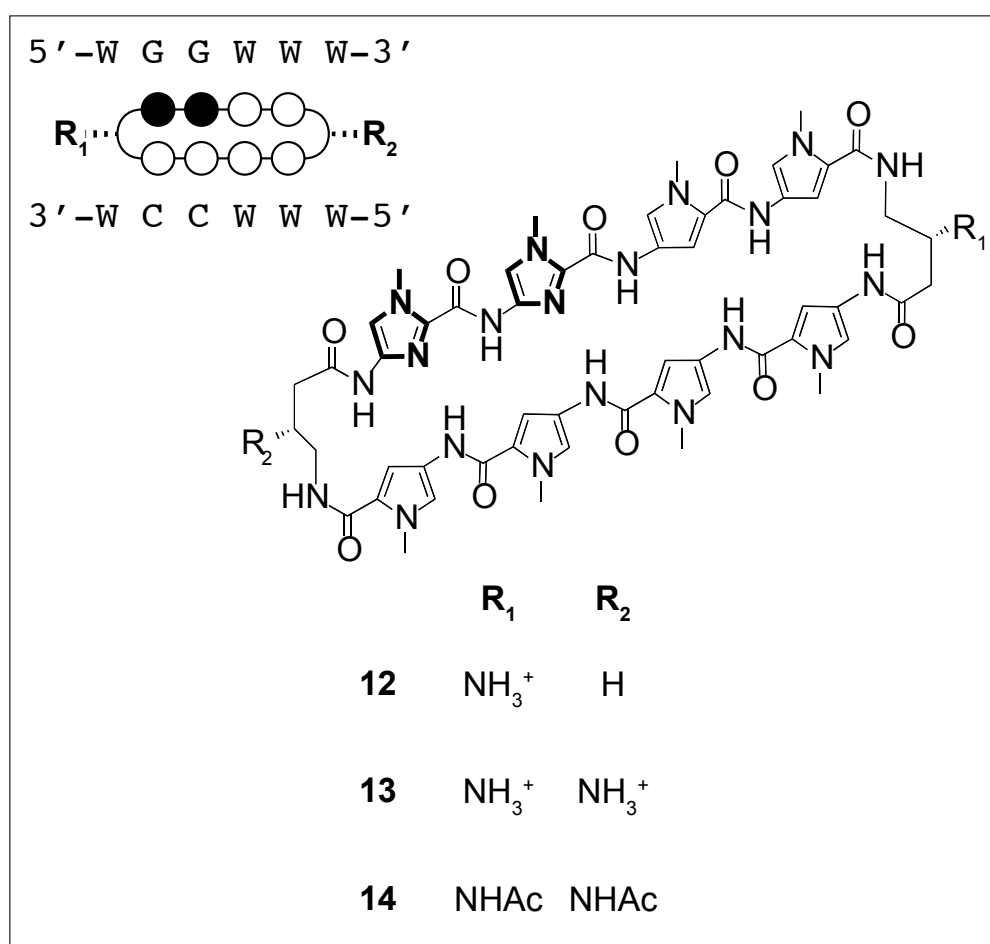


Figure 4.3: Chemical structures of cyclic polyamide library along with the corresponding circle-stick model and target DNA sequence. Legend: black circle = Im; white circle = Py; semi-circle = γ -aminobutyric acid unit with dashed (R , β) substituents; W = A/T bases.

Dynamic Light Scattering

The aggregation propensity of Py-Im polyamides was investigated through dynamic light scattering (DLS). Compounds **1-14** were studied at 1, 4, and 10 μM concentrations in a 0.1% DMSO/PBS solution in order to approximate the DMSO concentration and salt content present in cell culture experiments. Stock solutions (1000x) of each polyamide in DMSO were rapidly mixed with PBS, and the scattered light intensity was measured over the course of 10 minutes. The minimum concentration at which each compound was found to give a significant signal intensity (3x the buffer signal as per manufacturer guidelines), along with the respective particle sizes derived from a cumulant fit of the autocorrelation functions, are listed in Table 4.1.³³ Hairpin polyamides generally formed particles with radii of 70-200 nm at 4 μM concentration. One notable trend is that the benzamide substituted compounds (**4** and **10**) formed measurable particles at lower concentrations (1 μM vs. 4 μM) than their free amine counterparts (**2** and **8**). Polyamides containing fluorescein substituents (**5** and **6**) formed significantly larger particles when compared to the isophthalic acid conjugates (**2** and **4**), and compound **11** precipitated from the solution before particle size could be determined. Interestingly, cyclic polyamides **12-14** formed larger particles than the hairpin polyamides, with the bis- β -amino substituted cycle **13** forming the largest particles in this data set. Similar results were observed for a number of additional polyamides (Table S4.1), except for compounds containing three or four consecutive imidazole rings (**17**, **18**), which formed particles too large to be accurately measured (radii > 1 μM).

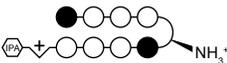
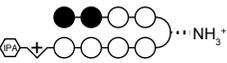
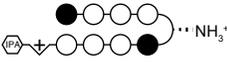
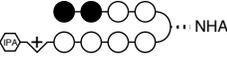
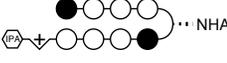
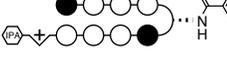
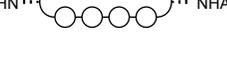
		Conc. (μM)	Radius (nm) ^a		Conc. (μM)	Radius (nm) ^a	
1		4	182 \pm 38	8		4	108 \pm 17
2		4	104 \pm 11	9		4	100 \pm 1
3		4	74 \pm 7	10		1	123 \pm 28
4		1	87 \pm 27	11		4	176 \pm 41
		4	127 \pm 32			-	n.d. ^b
5		1	294 \pm 67	12		4	197 \pm 28
6		1	147 \pm 40	13		4	347 \pm 113
7		4	124 \pm 19	14		4	182 \pm 14

Table 4.1: Estimated radii of polyamide aggregate particles at the concentration of minimum signal in 0.1% DMSO/PBS at 25 °C. ^aRadii derived from a cumulant fit of the average autocorrelation functions collected over 10 min. Errors represent standard deviation of at least three independent measurements. ^bRadius could not be determined due to rapid precipitation of the compound at 1 μM concentration.

Fractional Solubility Analysis

Next, the macroscopic solubility properties of these compounds were investigated by measuring the concentration of selected Py-Im polyamides in the soluble fraction of solutions with similar maximum concentrations (4 μM , Figure 4.4). Each compound was added as a 1000x (4 mM) stock in DMSO to PBS in accord with the light scattering experiments. Solutions were sonicated and then allowed to equilibrate for 2 hours at room temperature before aggregates were removed through centrifugation. In order to measure the concentration of polyamide in the supernatant, a plot of HPLC peak area vs. concentration was generated using polyamide 7 with detection at 310 nm, the wavelength at which each compound was quantified (Figure S4.1).

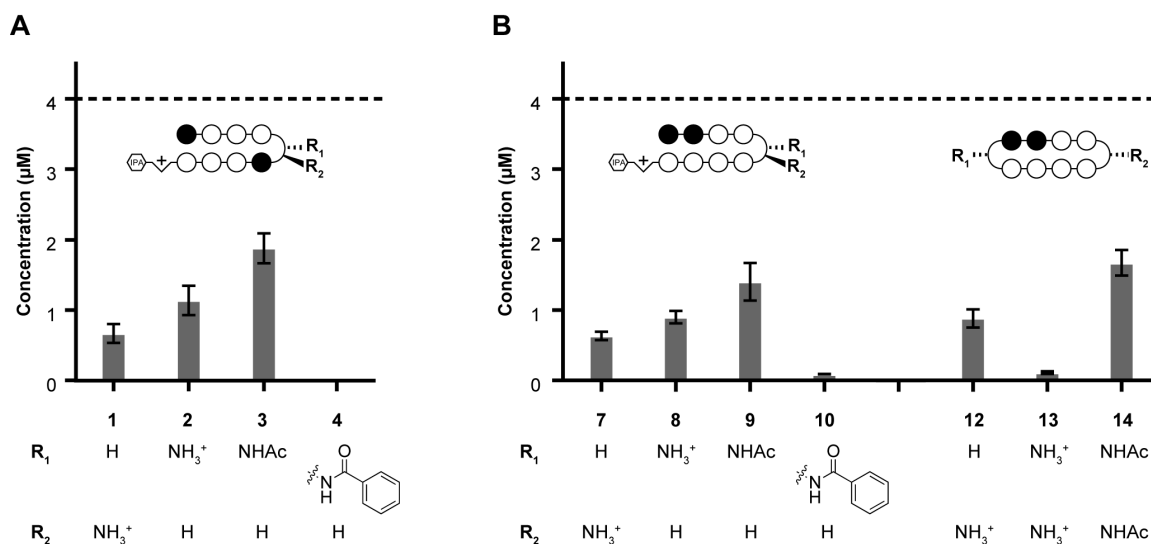


Figure 4.4: Calculated soluble concentration of select polyamides in 0.1% DMSO/PBS at 25°C. Maximum concentration estimated at 4 μM (dotted line) based on quantitation of starting material in 0.1% DMSO/water. Resultant concentrations determined by HPLC peak area at 310 nm detection after comparison with a standard curve (see SI). Error bars represent standard deviation of at least three independent measurements.

In general, the 5'-WGWWCW-3'-targeted hairpin polyamides (**1-4**) were found to be more soluble than their 5'-WGGWWW-3'-targeted counterparts (**7-10**). Within each set of polyamide hairpin cores, a relationship between turn substituents and solubility was observed. Polyamides with β -amine turns (**2**, **8**) were found to be more soluble than those compounds with α -amine-substituted turns (**1**, **7**), and the former compounds were further solubilized upon acetylation (**3**, **9**). Increased solubility upon incorporation of acetylated turn units was also observed in the cyclic architecture (**13** vs. **14**). The benzamide-substituted compounds (**4**, **10**) and the bis- β -amine substituted cycle **14** were found to be the least soluble, in good agreement with the light scattering measurements. Interestingly, none of the studied polyamides were fully soluble under these conditions.

Addition of Formulating Reagents

We thus decided to investigate the ability of known formulating reagents, in particular cyclodextrins (CDs),³⁴ to decrease aggregation and/or precipitation among the less soluble hairpin polyamides **7-10** (Figure 4.5). 2-Hydroxypropyl- β -cyclodextrin (Hp β CD) was chosen initially due to its high water solubility and low animal toxicity.³⁵ Using procedures identical to the solubility analyses, peak areas of Py-Im polyamides in the presence of 0, 5, or 50 mM Hp β CD were measured. A cyclodextrin-dependent increase of soluble polyamide concentration was observed for all compounds studied, with compounds **7** and **8** near the maximum expected concentration in solutions of 50 mM Hp β CD (Figure 4.5A). Impressively, 50 mM Hp β CD increased the concentration of the least soluble derivative (benzamide-substituted polyamide **10**) over 50-fold.

Surprisingly, the soluble concentration observed for polyamide **9** was significantly higher than expected based on the quantitation of the corresponding DMSO stock solution. This result likely derives from aggregation and/or precipitation of compound **9** upon dilution of the polyamide in water before the absorbance is measured, resulting in an underestimation of the stock concentration. We further probed the specificity of these effects by studying the solubilization of polyamide **7** by other carbohydrate formulating reagents, namely α -CD, γ -CD, hydroxypropyl methylcellulose (hypromellose), and dextrose (Figure S4.2). The three cyclodextrin derivatives were studied at 5 mM concentrations while hypromellose, a linear substituted glucose polymer, and dextrose, the glucose monomer, were normalized for total sugar content against 5 mM Hp β CD. In addition to Hp β CD, polyamide **7** was solubilized by γ -CD and hypromellose (Figure 4.5B).

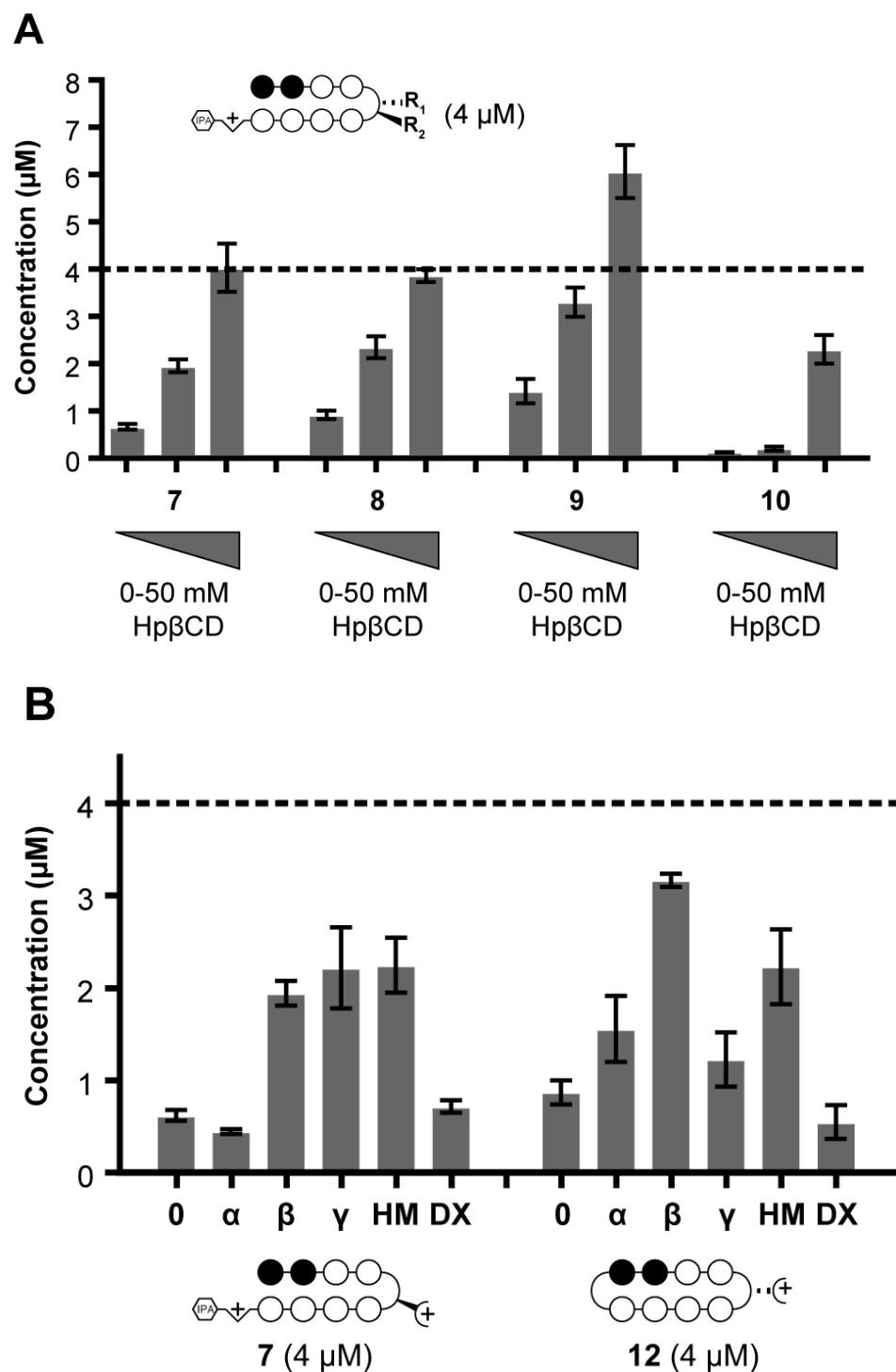


Figure 4.5: A) Calculated soluble concentration of polyamides 7 - 10 in 0.1% DMSO/PBS containing 0, 5, or 50 mM HP β CD at 25°C. B) Calculated soluble concentration of polyamides 7 and 12 in 0.1% DMSO/PBS containing: 5 mM α -, Hp β -, γ -cyclodextrin (α , β , γ , respectively); 6 mg/mL hypromellose (HM); 35 mM dextrose (DX). Maximum concentration estimated at 4 μM (dotted line) based on quantitation of starting material in 0.1% DMSO/water. Resultant concentrations determined by HPLC peak area ($\lambda = 310$ nm) after comparison with a standard curve (see SI). Error bars represent standard deviation of at least three independent measurements.

Polyamide **12**, which would seem less likely to form an inclusion complex with cyclodextrin due to its cyclic form, was screened against the same formulating agents. Hp β CD and hypromellose also solubilized cyclic compound **12**. Notably, neither polyamide displayed an increased solubility in the monomer (dextrose) solution.

Mouse Model Experiments

The utility of these results was further probed in an animal model system. Our laboratory recently found that high blood levels of polyamide **7** can be achieved in mice following an intraperitoneal (IP) injection of 120 nmol compound in a vehicle of 20% DMSO/PBS (600 μ M concentration, Figure 4.6A).¹⁸ Using Hp β CD, the DMSO content could be reduced to 1% with no loss in solubility. IP injections of 120 nmol polyamide **7** in a 1% DMSO/80 mM Hp β CD / PBS vehicle and the subsequent blood collection were performed under identical conditions to those previously reported. After blood collection, the plasma was isolated through centrifugation and the bulk proteins removed through methanol precipitation. The supernatant was then mixed with dilute aqueous trifluoroacetic acid (TFA) and a reference compound in acetonitrile was added. The injection vehicle containing Hp β CD yielded circulating polyamide concentrations comparable to those previously reported (Figure 4.6B). In both cases, polyamide concentrations of 13-14 μ M were detected in mouse plasma 1.5 hours after injection, with no polyamide detected after 24 hours. Furthermore, FITC-labeled compound **11**, which formed a precipitate in 20% DMSO/PBS solutions, was fully solubilized upon addition of Hp β CD (80 mM), allowing the compound to be injected into mice.

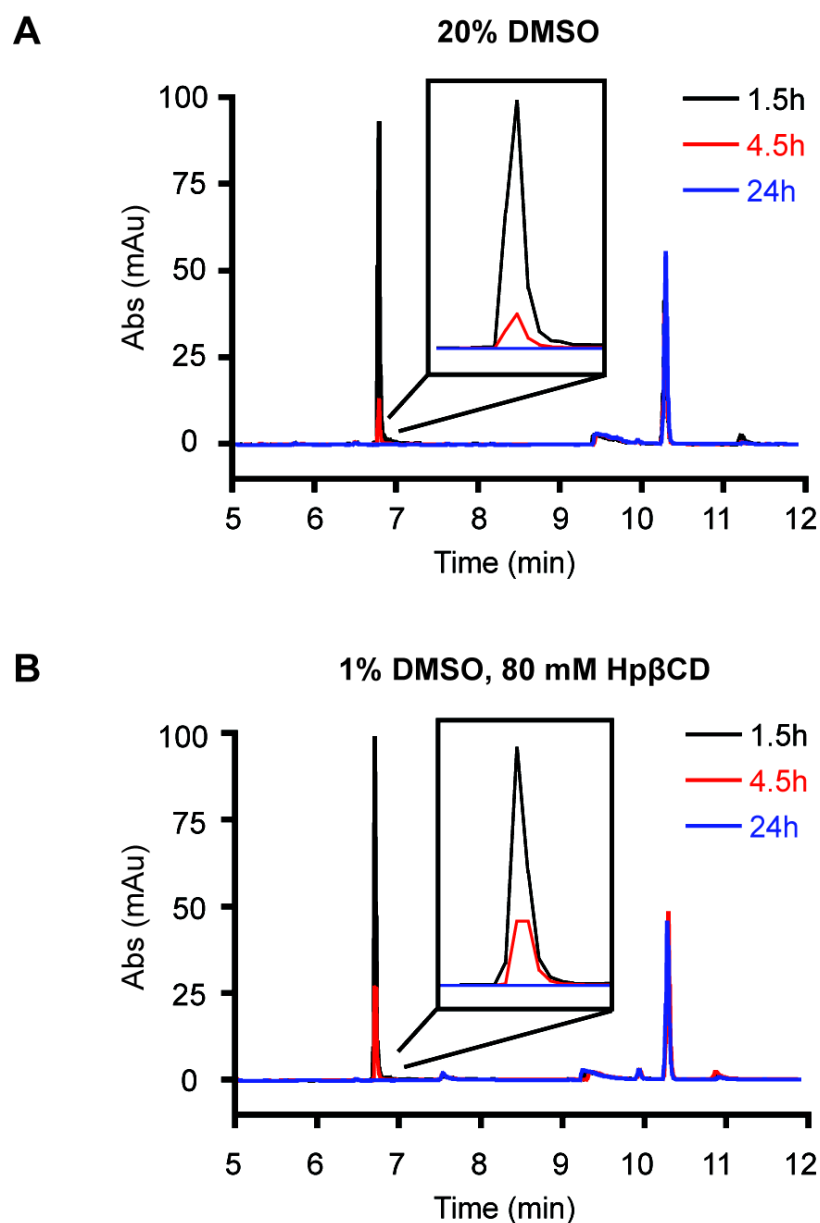


Figure 4.6: HPLC traces of mouse plasma isolated from four mice at three time points after injection with 120 nmol polyamide **7** in two different vehicles: 20% PBS / DMSO (A) and 1% DMSO/80 mM HP β CD / PBS (B).

Slightly reduced plasma concentrations of compound **11** were observed as compared to compound **7**, which may indicate reduced bioavailability of the FITC-modified polyamide (Figure 4.7A). We then sought to investigate the availability of the circulating polyamide to human cells by taking advantage of the nuclear staining generally observed with FITC-polyamide conjugates. Plasma samples isolated from mice

injected with compound **11** were added to A549 (human lung cancer) cells 16 hours prior to imaging live cells with confocal microscopy. In cells treated with plasma collected at 1.5 hours post-injection, strong nuclear fluorescent signals were observed (Figure 4.7B). Greatly reduced levels were observed with plasma isolated 4.5 hours post-injection, and no significant signal was observed with the addition of the 24 hours plasma sample (Figure 4.8).

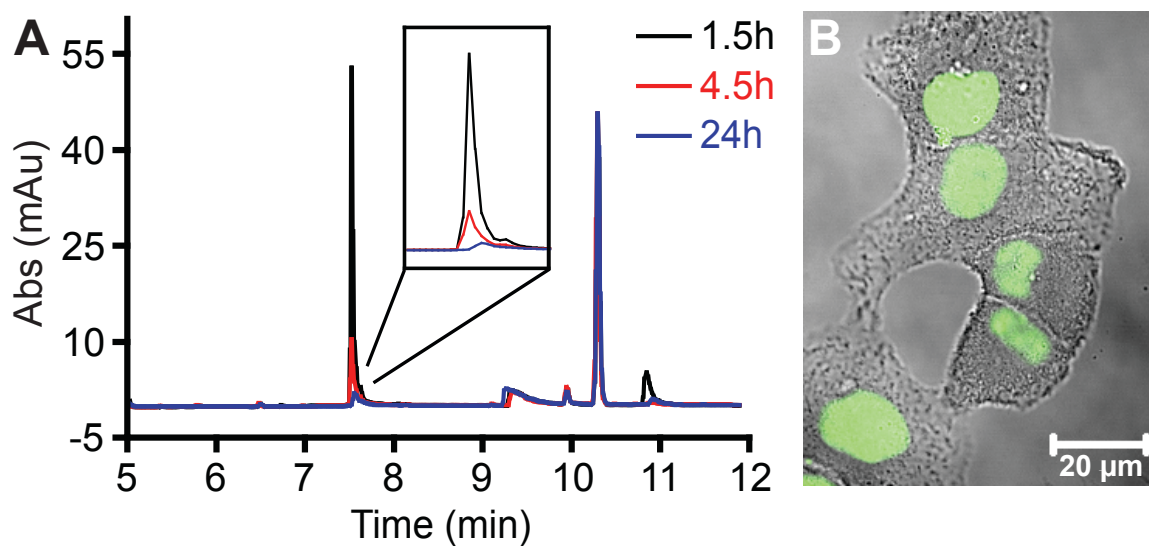


Figure 4.7: A) HPLC traces of mouse plasma isolated from four mice at three time points after injection with 120 nmol polyamide **11** in 20% DMSO/80 mM HP β CD / PBS. B) Confocal image of A549 cells after 16 hr incubation with mouse plasma isolated 1.5 hr after injection with polyamide **11**.

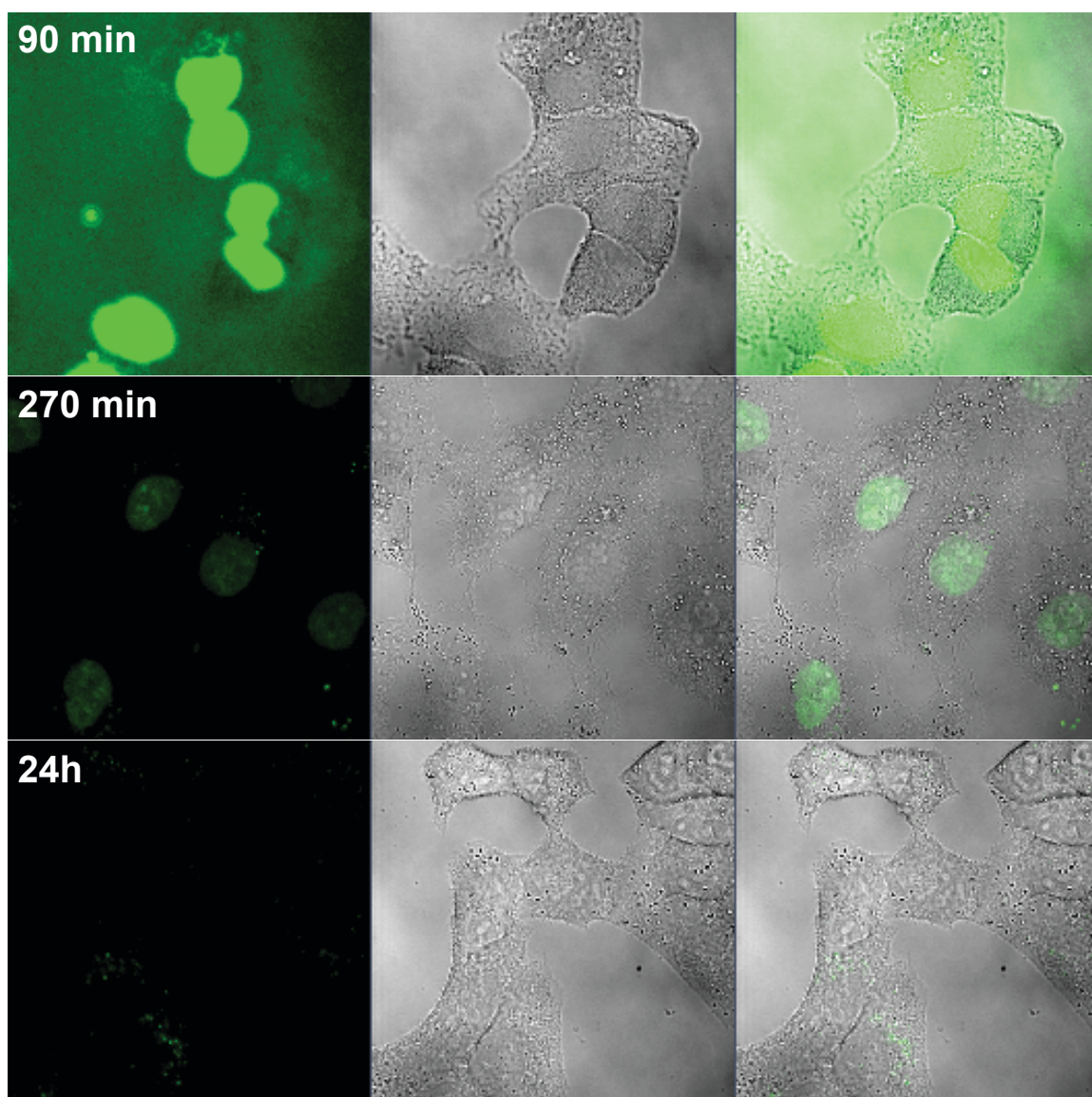


Figure 4.8: Confocal images of A549 cells after 16 hr incubation with mouse plasma isolated 90 min, 270 min, and 24 hr after injection with polyamide **11**. Images have been analyzed with identical intensity, brightness, and contrast settings to allow a direct comparison. Left: Fluorescence channel; Middle: Bright field image; Right: Overlay.

Conclusions

Dynamic light scattering measurements revealed that both hairpin and cyclic polyamides form measurable particles between 5 and 500 nm in size at biologically relevant concentrations (Table 4.1). Particle size was observed to be dependent on both cyclic vs. hairpin architecture and the terminal (tail) substituent. Interestingly, particles of similar size were observed for all polyamides containing an isophthalic acid (IPA) at the C-terminus despite the differing activities of these compounds in cell culture. These results support a mechanism of polyamide activity in which aggregation may not be a key factor.

Another interesting observation is that neither aggregation nor solubility is affected by the overall ionic charge of the polyamide. While organic compounds with ionizable groups are generally expected to be more soluble in aqueous salt solutions, neither light scattering nor solubility analyses revealed such a dependence. Indeed, hairpins and cycles in which the GABA amino turn units were modified with acetyl groups were found to be the most soluble.

At first glance, the lack of solubility observed for some polyamides is surprising as similar concentrations are commonly used in cell culture experiments, often without evidence of aggregation or precipitation. However, the experimental conditions required for the solubility experiments are a limited comparison to those in cell culture. For example, cell media generally contain a variety of small molecule and protein nutrients, and cell cultures are kept at higher temperatures (37 °C vs. 25 °C). In addition, the soluble fraction isolated by centrifugation is not necessarily representative of the available polyamide concentration during a typical cell incubation period (48-72 h),

particularly if aggregation is a dynamic process. We note that similar solubility problems have been reported by Sugiyama and co-workers, who enhanced the biological activity of seco-CBI polyamide conjugates through PEGylation³⁶ or liposomal formulations.³⁷

We were able to mitigate the problem of polyamide solubility through the addition of carbohydrate formulating reagents, in particular Hp β CD. As cyclodextrins are generally thought to form discrete inclusion complexes with small organic molecules,^{35,38} we postulated that the linear conformation of hairpin polyamides may be well solubilized by such additives. Indeed, the solubilization of polyamide **7** by the larger cyclodextrins (β and γ) is consistent with the formation of possible cyclodextrin inclusion complexes,³⁹ which in this case may result from interactions with the isophthalic acid unit at the C-terminus or the N-methylimidazole group at the N-terminus. Such interactions would not be expected, however, between cyclodextrins and cyclic polyamide **12**. Interestingly, solubilization of compound **12** was observed with Hp β CD but not the other cyclodextrin derivatives. The lack of solubilization with γ CD would be consistent with a model in which the interactions between Hp β CD and cycle **12** rely more on the hydroxypropyl substituents unique to Hp β CD, perhaps through additional hydrogen bonding interactions, rather than encapsulation. While both the linear **7** and cyclic **12** polyamide compounds were solubilized by hypromellose, presumably through encapsulation within the polymer matrix, it is notable that no significant solubilization was observed with the dextrose monomer. This latter observation may indicate the importance of an ordered carbohydrate structure, such as that available with cyclodextrins and hypromellose, for efficient polyamide solubilization. Further studies are necessary, however, before

conclusions can be drawn regarding the interactions between Py-Im polyamides and carbohydrate derivatives, and such investigations fall outside the scope of this work.

Further evidence of the utility of Hp β CD as a formulating reagent was gathered in mouse experiments. First, we demonstrated that the Hp β CD vehicle did not significantly affect circulating levels of polyamide **7**. On the other hand, the fluorescently labeled derivative **11** was only sufficiently soluble in Hp β CD solutions. As a result, hairpin **11** could be injected into mice using this vehicle. This tagged compound was of particular interest due to the high plasma protein binding levels (>99%) that had been previously reported for Py-Im polyamides during ADMET studies.²⁸ Evidence of nuclear uptake was observed in A549 cells following incubation with plasma from hairpin **11**-treated mice, thus demonstrating the availability of circulating polyamides to human cancer cells.

In summary, these studies have provided evidence that the aggregation propensity of Py-Im polyamides likely does not contribute to biological activity and may not be a critical concern in pharmacokinetic analyses. Solubility experiments revealed important trends, such as the increased solubility achieved by acetylation of the GABA amino turn unit, which will impact the design of next generation polyamides. Furthermore, the identification of an effective delivery vehicle will allow for the *in vivo* study of otherwise inaccessible Py-Im polyamides. These studies represent a valuable contribution to the field of small molecule transcriptional inhibitors and their ultimate utility as tools for perturbing gene expression networks *in vivo*.

Materials and Methods

Synthesis of Hairpin Py-Im Polyamides (1-11, 15-32)

The synthesis of Py-Im polyamides has been extensively described in previous work^{5,12,19,29,32} and is summarized as follows: Reagents were purchased from Sigma-Aldrich or Novabiochem. Py-Im cores were synthesized on Kaiser oxime resin using Boc-based chemistry, cleaved using 3,3'-diamino-N-methyldipropylamine, and purified by reverse phase preparative HPLC. The C-terminal amine was then derivatized with either isophthalic acid (IPA) or fluorescein isothiocyanate (FITC) and the crude intermediate isolated through ether precipitation. The GABA turn protecting groups (α -NHBoc or β -NHCBz) were removed under acidic conditions. If applicable, the crude intermediate was again isolated through ether precipitation and further derivatized at the GABA turn amine with either acetic anhydride or PyBOP-activated benzoic acid. Final products were purified through reverse phase HPLC and the identity confirmed through matrix-assisted laser desorption ionization – time-of-flight (MALDI-TOF) mass spectrometry. The synthesis and characterization of compounds **1**,¹⁰ **2-6**,¹⁹ **7**, **11**,¹² **15**, **25-32**¹⁹ were in line with literature reports. Results from MALDI-TOF characterization for compounds **8-10**, **12-14**, and **16-24** are available (Table S4.2).

Synthesis of Cyclic Py-Im Polyamides (12-14)

The synthesis and characterization of polyamides **12** and **13** have been previously described.¹⁸ In brief, the heterocyclic cores of these polyamides were synthesized on Kaiser oxime resin as above, except that a terminal GABA turn unit (Boc-GABA-OH or (R)-4-(Boc-amino)-3-(Z-amino)butyric acid) was added. Following deprotection of the

terminal Boc unit, the core was cleaved from the resin with DBU / H₂O and the resulting acid purified by reverse phase HPLC. The precursor acid was then cyclized using diphenylphosphorylazide under basic conditions. The crude intermediate was isolated through ether precipitation and the Cbz group(s) removed as above. Polyamides **12** and **13** were then isolated through reverse phase preparative HPLC. Polyamide **14** was synthesized by reaction of **13** with acetic anhydride under basic conditions and then purified by reverse phase HPLC. Results from MALDI-TOF characterization for compound **14** are available (Table S4.2).

Polyamide Quantification

Polyamide concentrations were measured by UV-absorption analysis on an Agilent 8453 diode array spectrophotometer in distilled and deionized water containing up to 0.1% DMSO using a molar extinction coefficient (ϵ) of 69,500 M⁻¹cm⁻¹ at 310 nm.

Dynamic Light Scattering

DMSO and PBS were passed through a 0.02 μ M syringe filter (Whatman) immediately prior to use. Stock solutions of each polyamide in DMSO were quantified as above and the purity determined by HPLC to be greater than 95%. Solutions of 1, 4, and 10 mM in DMSO were prepared and then centrifuged for 15 min at 16 x g to remove particulates. Immediately before measurement, 0.5 μ L of the DMSO stock was added to 500 μ L of PBS in a microcentrifuge tube. The solution was mixed briefly with a pipette tip and transferred to a disposable plastic cuvette (Fisher). Measurements were performed on a Wyatt Dynapro Nanostar instrument using a 659 nm / 100 mW laser at

100% power and a 90 degree detection angle at 25°C. Acquisition times of 10-15 sec were collected over 10 minutes and analyzed using the cumulant fit tool in the Dynamics (6.11.1.3) software with PBS as the referenced solvent. Acquisitions in which the baseline value of the fit was greater than ± 0.1 were omitted and the remaining traces averaged. Measurements in which the intensity (cts/s) was less than 3x the buffer signal intensity were considered below the detection limit.

Solubility Analysis

Stock solutions of each polyamide in DMSO were quantified as above and the purity checked by HPLC. Solutions of 4 mM stock were prepared in DMSO. Polyamide (0.5 μ L) was added to 500 μ L PBS in a microcentrifuge tube, and the solution was immediately vortexed and placed in a sonicating water bath at 25°C for 20 min. The tubes were then removed from the bath and allowed to equilibrate for 2 hr at room temperature. Samples were centrifuged for 20 min at 16 xg and 100 μ L of the supernatant removed for HPLC analysis. Analytical HPLC analysis was conducted on a Beckman Gold instrument equipped with a Phenomenex Gemini analytical column (250 x 4.6 mm, 5 μ m) and a diode array detector (Mobile phase: 10-80% CH₃CN in 0.1% CF₃CO₂H (aqueous) over 17.5 min; Flow rate: 1.50 mL / min; Injection volume: 40 μ L). Peaks were detected and integrated at 310 nm absorbance using the Karat32 software. Sample concentrations were determined through comparison to a standard curve of concentration vs. peak area that was generated using compound 7 (Figure S1). Solubilization by formulating agents proceeded similarly except that the DMSO stock solutions were added to PBS containing 5 or 50 mM Hp β CD, 5 mM α CD, 5 mM γ CD,

35 mM dextrose, or 6.00 mg / mL hypromellose (approximately 35 mM relative glucose units based on reported substitution for Aldrich lot #128k0214v).

Animal Experiments

Murine experiments were performed as described previously.¹⁸ In brief, C57bl/6 mice (8 to 12 weeks of age, Jackson Laboratory) were injected intraperitoneally with 200 μ L of a PBS solution containing: a) 120 nmol compound **7**, 20% DMSO; b) 120 nmol compound **7**, 1% DMSO, 80 mM Hp β CD; or c) 120 nmol compound **11**, 20% DMSO, 80 mM Hp β CD. Blood was collected from anesthetized animals (2-5% isoflurane) by retro-orbital withdrawal. Immediately after the third blood draw, animals were euthanized by asphyxiation in a CO₂ chamber (2 atm).

Plasma was isolated by centrifugation of the collected blood. The samples from the four replicate mice were combined at 5 μ L / sample, yielding 20 μ L combined plasma that was then treated with 40 μ L CH₃OH, vortexed, and centrifuged. Fifty μ L of the supernatant were combined with one equivalent of the HPLC loading solution (4:1 water/CH₃CN, 0.08 % CF₃CO₂H) containing Boc-Py-OMe (methyl 4-((tert-butoxycarbonyl)amino)-1-methyl-pyrrole-2-carboxylate) as an internal spike-in control. Analytical HPLC analyses were conducted with a Phenomenex Kinetex C18 analytical column (100 \times 4.6 mm, 2.6 μ m, 100 Å) and a diode array detector (Mobile phase: 5-60% CH₃CN in 0.1% (v/v) aqueous CF₃CO₂H over 12.5 min; Flow rate: 2.0 mL / min; Injection volume: 40 μ L). Peaks were detected and integrated at 310 nm absorbance, and sample concentrations were determined through comparison to the previously published standard curve for this column.¹⁸

Confocal Microscopy

For confocal microscopy experiments, A549 cells in F-12K medium supplemented with 10% FBS (1 mL, 100k cells / mL) were applied to culture dishes equipped with glass bottoms for direct imaging (MatTek). Cells were allowed to adhere for 18 hr in a 5% CO₂ atmosphere at 37 °C. The medium was then removed and replaced with 200 µl of fresh medium supplemented with 20 µL of plasma collected 1.5, 4.5, or 24 hr after injection of compound **11**. After an additional 16 hr incubation period, 100 µL of untreated medium was added to each slide prior to imaging. Imaging was performed at the Caltech Beckman Imaging Center using a Zeiss LSM 5 Pascal inverted laser scanning microscope equipped with a 63x oil-immersion objective lens. Fluorescence and visible-light images were obtained using standard filter sets for fluorescein and analyzed using Zeiss LSM software.

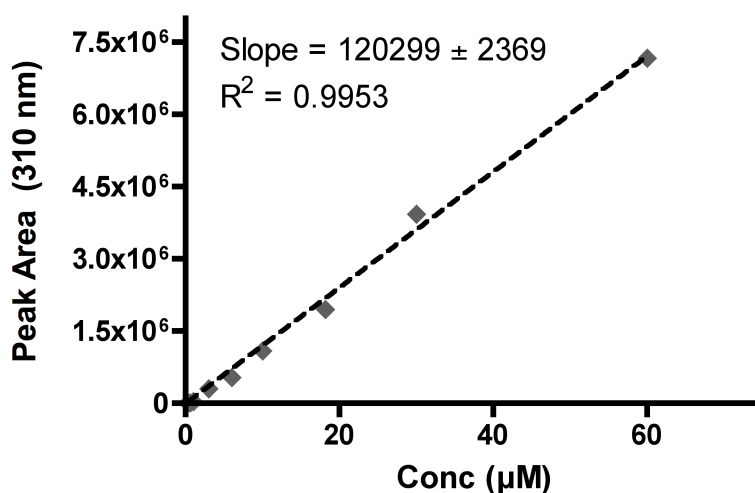


Figure S4.1. Plot of concentration vs. peak area plot derived from HPLC traces of compound **7** at 310 nm. Points were fit to a first order polynomial using the Prism software program (dotted line).

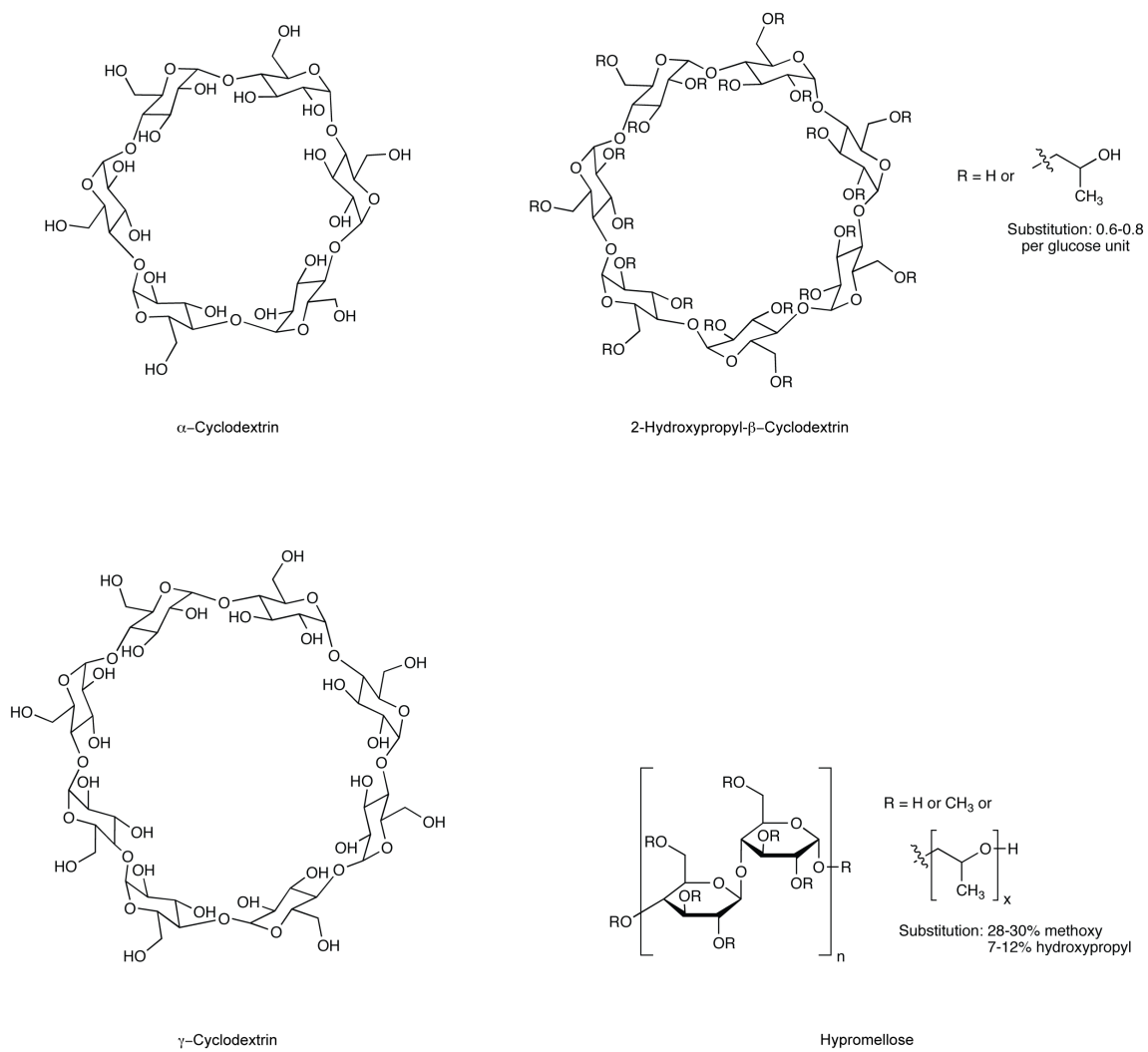


Figure S4.2. Structures of carbohydrate solubilizing agents.

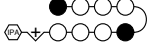
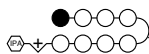
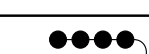
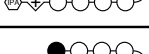
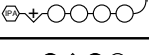
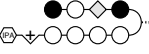
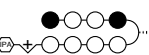
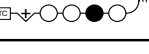
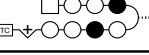
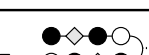
	Radius (nm) ^a				Intensity (cts/s)	
	Conc (μM)	Average	Std. Dev.	Average	Std. Dev.	
0.1% DMSO / PBS	-	-	-	-	2.2E+05	7.9E+04
	15	4	157	33	4.6E+06	2.0E+06
	16	4	128	11	5.1E+06	2.2E+06
	17	4	> 1000 ^b	-	3.5E+06	1.2E+06
	18	4	> 1000 ^b	-	4.8E+06	1.2E+06
	19	4	90	20	1.5E+06	9.3E+05
	20	10	111	13	1.0E+06	7.4E+05
	21	4	108	2	6.1E+06	3.1E+06
	22	4	123	8	6.0E+06	4.5E+04
	23	4	189	2	7.9E+06	2.4E+05
	24	10	100	12	8.7E+05	1.3E+05
	25	1	344	41	4.4E+06	1.4E+05
	26	1	112	8	8.7E+06	2.3E+05
	27	1	119	10	7.7E+06	5.3E+05
	28	1	132	5	2.4E+06	6.8E+05
	29	1	100	1	1.9E+06	1.9E+05
	30	4	101	4	5.8E+06	1.6E+06
	31	10	120	7	9.9E+05	2.9E+05
	32	10	99	2	7.7E+05	3.6E+04

Table S4.1: Estimated radii of polyamide aggregate particles at the concentration of minimum signal in 0.1% DMSO/PBS at 25 °C. *a.* Radii derived from a cumulant fit of the average autocorrelation functions Collected over 10 min. *b.* Compounds formed particles with radii too large to be accurately determined with this method (radius > 1 μM).

	Technique	Formula	Calculated Mass	Measured Mass (m/z)
8	MALDI-TOF	C ₆₅ H ₇₇ N ₂₂ O ₁₂	[M+H] ⁺ 1357.6	1357.8
9	MALDI-TOF	C ₆₇ H ₇₉ N ₂₂ O ₁₃	[M+H] ⁺ 1399.6	1399.8
10	MALDI-TOF	C ₇₂ H ₈₁ N ₂₂ O ₁₃	[M+H] ⁺ 1461.6	1461.8
14	MALDI-TOF	C ₅₈ H ₆₇ N ₂₂ O ₁₂	[M+H] ⁺ 1263.5	1263.9
16	MALDI-TOF	C ₆₆ H ₇₈ N ₂₁ O ₁₂	[M+H] ⁺ 1356.6	1356.6
17	MALDI-TOF	C ₆₄ H ₇₆ N ₂₃ O ₁₂	[M+H] ⁺ 1358.6	1358.8
18	MALDI-TOF	C ₆₃ H ₇₅ N ₂₄ O ₁₂	[M+H] ⁺ 1359.6	1360.0
19	MALDI-TOF	C ₆₆ H ₇₈ N ₂₁ O ₁₂	[M+H] ⁺ 1356.6	1356.8
20	MALDI-TOF	C ₆₂ H ₇₆ N ₂₁ O ₁₂	[M+H] ⁺ 1306.6	1306.9
21	MALDI-TOF	C ₆₂ H ₇₆ N ₂₁ O ₁₂	[M+H] ⁺ 1306.6	1307.3
22	MALDI-TOF	C ₆₅ H ₇₇ N ₂₂ O ₁₂	[M+H] ⁺ 1357.6	1357.8
23	MALDI-TOF	C ₆₅ H ₇₇ N ₂₂ O ₁₂	[M+H] ⁺ 1357.6	1358.0
24	MALDI-TOF	C ₆₂ H ₇₆ N ₂₁ O ₁₂	[M+H] ⁺ 1306.6	1306.9

Table S4.2. Mass spectroscopy results for unpublished compounds **8-10, 12-14, 16-24**.

Acknowledgements

We thank Dr. Jennifer Keefe (California Institute of Technology) and Sigrid Kuebler (Wyatt Technology Corporation) for assistance with DLS experimentation and data analysis and Dr. Adam Urbach (Trinity University) for helpful discussions. A.E.H. thanks the California Tobacco-Related Disease Research Program (19FT-0105) and the NIH (NRSA number 1F32CA156833) for postdoctoral support. J.A.R. is grateful to the Alexander von Humboldt foundation for the award of a Feodor Lynen postdoctoral fellowship. J.L.M. acknowledges the American Cancer Society for a postdoctoral fellowship (PF-10-015-01-CDD). D.C.M. thanks the National Institutes of Health for a Cellular, Biochemical, and Molecular Sciences Predoctoral Research training grant (5T32GM007616). This work was supported by the Ellison Medical Foundation (AG-SS-2256-09) and NIH grants (GM27681, GM51747).

References

1. Dervan, P. B., Molecular recognition of DNA by small molecules. *Bioorg. Med. Chem.* **2001**, 9, 2215-2235.
2. Dervan, P. B.; Edelson, B. S., Recognition of the DNA minor groove by pyrrole-imidazole polyamides. *Curr. Opin. Struct. Biol.* **2003**, 13, 284-299.
3. Hsu, C. F.; Dervan, P. B., Quantitating the concentration of Py-Im polyamide-fluorescein conjugates in live cells. *Bioorg. Med. Chem. Lett.* **2008**, 18, 5851-5855.
4. Edelson, B. S.; Best, T. P.; Olenyuk, B.; Nickols, N. G.; Doss, R. M.; Foister, S.; Heckel, A.; Dervan, P. B., Influence of structural variation on nuclear localization of DNA-binding polyamide-fluorophore conjugates. *Nucleic Acids Res.* **2004**, 32, 2802-2818.
5. Nickols, N. G.; Jacobs, C. S.; Farkas, M. E.; Dervan, P. B., Improved nuclear localization of DNA-binding polyamides. *Nucleic Acids Res.* **2007**, 35, 363-370.
6. Chenoweth, D. M.; Dervan, P. B., Allosteric modulation of DNA by small molecules. *Proc. Natl. Acad. Sci. USA* **2009**, 106, 13175-13179.
7. Chenoweth, D. M.; Dervan, P. B., Structural Basis for Cyclic Py-Im Polyamide Allosteric Inhibition of Nuclear Receptor Binding. *J. Am. Chem. Soc.* **2010**, 132, 14521-14529.
8. Nickols, N. G.; Dervan, P. B., Suppression of androgen receptor-mediated gene expression by a sequence-specific DNA-binding polyamide. *Proc. Natl. Acad. Sci. USA* **2007**, 104, 10418-10423.
9. Nickols, N. G.; Jacobs, C. S.; Farkas, M. E.; Dervan, P. B., Modulating hypoxia-inducible transcription by disrupting the HIF-1-DNA interface. *ACS Chemical Biology.* **2007**, 2, 561-571.
10. Muzikar, K. A.; Nickols, N. G.; Dervan, P. B., Repression of DNA-binding dependent glucocorticoid receptor-mediated gene expression. *Proc. Natl. Acad. Sci. USA* **2009**, 106, 16598-16603.
11. Olenyuk, B. Z.; Zhang, G.-J.; Klco, J. M.; Nickols, N. G.; Kaelin, W. G., Jr.; Dervan, P. B., Inhibition of vascular endothelial growth factor with a sequence-specific hypoxia response element antagonist. *Proc. Natl. Acad. Sci. USA* **2004**, 101, 16768-16773.
12. Raskatov, J. A.; Meier, J. L.; Puckett, J. W.; Yang, F.; Ramakrishnan, P.; Dervan, P. B., Modulation of NF-kappaB-dependent gene transcription using programmable DNA minor groove binders. *Proc. Natl. Acad. Sci. USA* **2012**, 109, 1023-1028.
13. Takahashi, T.; Asami, Y.; Kitamura, E.; Suzuki, T.; Wang, X.; Igarashi, J.; Morohashi, A.; Shinojima, Y.; Kanou, H.; Saito, K.; Takasu, T.; Nagase, H.; Harada, Y.; Kuroda, K.; Watanabe, T.; Kumamoto, S.; Aoyama, T.; Matsumoto, Y.; Bando, T.; Sugiyama, H.; Yoshida-Noro, C.; Fukuda, N.; Hayashi, N., Development of pyrrole-

imidazole polyamide for specific regulation of human aurora kinase-A and -B gene expression. *Chem. Biol.* **2008**, 15, 829-841.

14. Yao, E.-H.; Fukuda, N.; Ueno, T.; Matsuda, H.; Nagase, H.; Matsumoto, Y.; Sugiyama, H.; Matsumoto, K., A pyrrole-imidazole polyamide targeting transforming growth factor-beta1 inhibits restenosis and preserves endothelialization in the injured artery. *Cardiovasc. Res.* **2009**, 81, 797-804.

15. Matsuda, H.; Fukuda, N.; Ueno, T.; Katakawa, M.; Wang, X.; Watanabe, T.; Matsui, S.; Aoyama, T.; Saito, K.; Bando, T.; Matsumoto, Y.; Nagase, H.; Matsumoto, K.; Sugiyama, H., Transcriptional inhibition of progressive renal disease by gene silencing pyrrole-imidazole polyamide targeting of the transforming growth factor-beta1 promoter. *Kidney Int.* **2011**, 79, 46-56.

16. Chenoweth, D. M.; Harki, D. A.; Phillips, J. W.; Dose, C.; Dervan, P. B., Cyclic pyrrole-imidazole polyamides targeted to the androgen response element. *J. Am. Chem. Soc.* **2009**, 131, 7182-7188.

17. Harki, D. A.; Satyamurthy, N.; Stout, D. B.; Phelps, M. E.; Dervan, P. B., In vivo imaging of pyrrole-imidazole polyamides with positron emission tomography. *Proc. Natl. Acad. Sci. USA* **2008**, 105, 13039-13044.

18. Raskatov, J. A.; Hargrove, A. E.; So, A. Y. Dervan, P. B., Pharmacokinetics of Py-Im polyamides depend on architecture: cyclic versus linear. *J. Am. Chem. Soc.* **2012**, 134, 7995-7999.

19. Meier, J. L.; Montgomery, D. C.; Dervan, P. B., Enhancing the cellular uptake of Py-Im polyamides through next-generation aryl turns. *Nucleic Acids Res.* **2011**, 40, 2345-2356.

20. McGovern, S. L.; Helfand, B. T.; Feng, B.; Shoichet, B. K., A specific mechanism of nonspecific inhibition. *J. Med. Chem.* **2003**, 46, 4265-4272.

21. Feng, B. Y.; Shelat, A.; Doman, T. N.; Guy, R. K.; Shoichet, B. K., High-throughput assays for promiscuous inhibitors. *Nat. Chem. Biol.* **2005**, 1, 146-148.

22. Coan, K. E. D.; Shoichet, B. K., Stability and equilibria of promiscuous aggregates in high protein milieus. *Mol. BioSyst.* **2007**, 3, 208-213.

23. Coan, K. E. D.; Shoichet, B. K., Stoichiometry and physical chemistry of promiscuous aggregate-based inhibitors. *J. Am. Chem. Soc.* **2008**, 130, 9606-9612.

24. Feng, B. Y.; Simeonov, A.; Jadhav, A.; Babaoglu, K.; Inglese, J.; Shoichet, B. K.; Austin, C. P., A high-throughput screen for aggregation-based inhibition in a large compound library. *J. Med. Chem.* **2007**, 50, 2385-2390.

25. Shoichet, B. K.; Seidler, J.; McGovern, S. L.; Doman, T. N., Identification and prediction of promiscuous aggregating inhibitors among known drugs. *J. Med. Chem.* **2003**, 46, 4477-4486.

26. Frenkel, Y. V.; Clark, A. D., Jr.; Das, K.; Wang, Y. H.; Lewi, P. J.; Janssen, P. A.; Arnold, E., Concentration and pH dependent aggregation of hydrophobic drug molecules and relevance to oral bioavailability. *J. Med. Chem.* **2005**, *48*, 1974-1983.
27. Doak, A. K.; Wille, H.; Prusiner, S. B.; Shoichet, B. K., Colloid formation by drugs in simulated intestinal fluid. *J. Med. Chem.* **2010**, *53*, 4259-4265.
28. Chenoweth, D. M.; Harki, D. A.; Phillips, J. W.; Dose, C.; Dervan, P. B., Cyclic pyrrole-imidazole polyamides targeted to the androgen response element. *J. Am. Chem. Soc.* **2009**, *131*, 7182-7188.
29. Dose, C.; Farkas, M. E.; Chenoweth, D. M.; Dervan, P. B., Next generation hairpin polyamides with (R)-3,4-diaminobutyric acid turn unit. *J. Am. Chem. Soc.* **2008**, *130*, 6859-6866.
30. Jacobs, C. S.; Dervan, P. B., Modifications at the C-terminus to improve pyrrole-imidazole polyamide activity in cell culture. *J. Med. Chem.* **2009**, *52*, 7380-7388.
31. Herman, D. M.; Turner, J. M.; Baird, E. E.; Dervan, P. B., Cycle polyamide motif for recognition of the minor groove of DNA. *J. Am. Chem. Soc.* **1999**, *121*, 1121-1129.
32. Belitsky, J. M.; Nguyen, D. H.; Wurtz, N. R.; Dervan, P. B., Solid-phase synthesis of DNA binding polyamides on oxime resin. *Bioorg. Med. Chem.* **2002**, *10*, 2767-2774.
33. Dynamics Software Package (6.11.13), Wyatt Technologies.
34. Loftsson, T.; Brewster, M. E., Pharmaceutical applications of cyclodextrins: basic science and product development. *J. Pharm. Pharmacol.* **2010**, *62*, 1607-1621.
35. Gould, S.; Scott, R. C., 2-hydroxypropyl-beta-cyclodextrin (HP-beta-CD): A toxicology review. *Food Chem. Toxicol.* **2005**, *43*, 1451-1459.
36. Takagaki, T.; Bando, T.; Kitano, M.; Hashiya, K.; Kashiwazaki, G.; Sugiyama, H., Evaluation of PI polyamide conjugates with eight-base pair recognition and improvement of the aqueous solubility by PEGylation. *Bioorg. Med. Chem.* **2011**, *19*, 5896-5902.
37. Kashiwazaki, G.; Bando, T.; Yoshidome, T.; Masui, S.; Takagaki, T.; Hashiya, K.; Pandian, G. N.; Yasuoka, J.; Akiyoshi, K.; Sugiyama, H., Synthesis and biological properties of highly sequence-specific-alkylating N-methylpyrrole, N-methylimidazole polyamide conjugates. *J. Med. Chem.* **2012**, *55*, 2057-2066.
38. Szejtli, J., Introduction and general overview of cyclodextrin chemistry. *Chem. Rev.* **1998**, *98*, 1743-1753.
39. Loftsson, T.; Brewster, M. E., Pharmaceutical applications of cyclodextrins. 1. Drug solubilization and stabilization. *J. Pharm. Sci.* **1996**, *85*, 1017-1025.